UDK 669.14.018.8:621.791:543.456
Original scientific article/Izvirni znanstveni članek

ISSN 1580-2949
Mater. Tehnol.

OPTIMIZING WELD QUALITY IN DISSIMILAR STAINLESS STEEL JOINTS FOR INDUSTRIAL APPLICATIONS

OBLIKOVANJE KVALITETNIH INDUSTRIJSKIH ZVAROV PRI SPAJANJU NERJAVNIH JEKEL Z RAZLIČNO KEMIJSKO SESTAVO

D. Selvamuthukumaran[1], V. C. Uvaraja[2]

[1]Department of Mechanical Engineering, Bannari Amman Institute of Technology, Sathyamangalam, Erode 638401, India
[2]Department of Agricultural Engineering, Bannari Amman Institute of Technology, Sathyamangalam, Erode 638401, India

Prejem rokopisa – received: 2024-08-28; sprejem za objavo – accepted for publication: 2024-11-07

doi:10.17222/mit.2024.1288

The research aims to develop quality joints using cold metal transfer (CMT) welding. We investigated stainless steel sheets such as Duplex 2205, SS 301 LN and ER 308L SS filler wire used for chemical and food processing equipment applications. The major focus was on optimizing the welding parameters for producing quality weld joints, thus ensuring the optimal ultimate tensile strength (UTS) and microhardness ($HV_{0.5}$). The Taguchi L9 orthogonal array was used in this study to find the most significant parameters among welding speed (S), current (A) and contact-to-work distance (CTWD), and their optimum settings for producing high-quality welds. The multi-objective optimization TOPSIS method was employed to optimize the ultimate tensile strength (UTS) and microhardness ($HV_{0.5}$). According to the TOPSIS performance index, the welding current was identified as the most influential factor, contributing 94.79 %, followed by welding speed and CTWD contributing 4.48 % and 0.15 %, respectively. The optimized welding parameters including a current of 95 A, welding speed (travel speed) of 4 mm/sec, and CTWD of 5 mm were identified as the best results. Confirmatory experiments were conducted to validate the optimized settings; they demonstrated good agreement with the predicted results. Finally, optical microscopy (OM), scanning electron microscopy (SEM) and energy-dispersive X-ray spectroscopy (EDXS) analyses of the optimal weld microstructure were presented.

Keywords: dissimilar stainless steel, cold metal transfer (CMT) welding, Taguchi L9 optimization, TOPSIS, ultimate tensile strength (UTS), microhardness ($HV_{0.5}$), scanning electron microscopy (SEM), energy-dispersive X-ray spectroscopy (EDXS)

V članku avtorji opisujejo raziskavo, katere namen je bil razviti kvalitetne zvarne spoje s postopkom prenosa taline na hladno kovino (CMT; angl.: Cold Metal Transfer). Raziskavo so izvajali z medsebojnim zvarjanjem pločevine iz nerjavnih jekel z različno kemijsko sestavo; kot sta v tem primeru Duplex 2205 in SS 301 LN. Ti dve jekli se uporabljata za izdelavo opreme v kemijski in procesni industriji. Izbrana polnilna žica za navarjanje s CTM postopkom je bila iz nerjavnega jekla vrste ER 308L SS. Avtorji so se v raziskavi osredotočili predvsem na optimiziranje parametrov CTM procesa, ki zagotavljajo izdelavo kvalitetnih zvarnih spojev s predpisano končno natezno trdnostjo (UTS; angl.: ultimate tensile strength) in mikrotrdoto (HV; Vickers microhardness). Zato, da bi določili najbolj pomembne vplivne procesne parametre CTM postopka so uporabili Taguchijevo ortogonalno matrico L9. Izbrani procesni parametri, ki so jih zasledovali so bili hitrost navarjanja (S), jakost električnega toka (A) in kontaktna delovna razdalja (CTWD; angl.: contact-to-work distance). Avtorji so uporabili več objektno (več kriterijsko) optimizacijsko tehniko (TOPSIS; angl.: multiobjective optimization technique) za optimiziranje končne natezne trdnosti in mikrotrdote izdelanih zvarnih spojev. Na osnovi dobljenih TOPSIS performančnih indeksov so ugotovili, da je jakost električnega toka najvplivnejši procesni parameter izbranega CMT postopka spajanja. Ta prispeva 94,79 %, medtem, ko je prispevek hitrosti varjenja le 4,48 %-ten in CTWD 0,15 %-en. Najboljše lastnosti zvarnih spojev izdelanih s CMT spajanjem med izbranima vrstama nerjavnih jekel so dosegli pri jakosti električnega toka 95 A, hitrosti potovanja elektrode 4 mm/sek., in CTWD 5 mm. Z optimizacijsko metodo napovedani rezultati so se dobro ujemali z eksperimentalnimi rezultati. Na koncu so avtorji v članku predstavili še optimalne mikrostrukture zvarnih spojev, izdelanih s pomočjo optične (OM) in vrstične elektronske mikroskopije (SEM) ter mikrokemijskih analiz s pomočjo spektroskopije na osnovi spektroskopije z disperzijo energije rentgenskih žarkov (EDXS; angl.: Energy-dispersive X-ray spectroscopy).

Ključne besede: nerjavna jekla z različno kemijsko sestavo, varjenje s prenosom taline na hladno kovino, Taguchi optimizacija L9, več kriterijska optimizacijska tehnika TOPSIS, končna natezna trdnost, Vickersova mikrotrdota, vrstična elektronska mikroskopija, spektroskopija na osnovi disperzije energije rentgenskih žarkov.

1 INTRODUCTION

Duplex stainless steel (2205) (DSS) is gaining attraction in the stainless steel market, driven by two key factors such as nickel volatility and superior performance. Low nickel volatility provides a low-nickel alternative, making it more cost-effective and resilient to market fluctuations. It also boasts impressive corrosion resistance in harsh environments, outperforming many ASS grades. This makes it ideal for demanding applications like vehicle building shipbuilding, chemical processing, and desalination plants.[1] Cold-rolled 301LN plates, with yield strengths ranging from 200 MPa to 700 MPa and the ability to undergo strain-induced martensite transformation, are an excellent standard for lightweight railway passenger car and vehicle bodies, effortlessly meeting all strength requirements.[2] Duplex stainless steels (DSS) are poised for future growth due to their advantages, but austenitic stainless steels (ASS) still dominate the market with a 70 % share. As a result, combinations of both ma-

*Corresponding author's e-mail:
selvamuthukumaran@bitsathy.ac.in (D. Selvamuthukumaran)

terials are used in demanding environments, like Matsuyama's water tank using DSS, 304 ASS, and 316 ASS.[3] The weldability of Duplex 2205 with 301LN is limited in most welding processes. Due to the wide applications of these two materials, researchers have investigated the process extensively. However, these materials are challenging to weld because of differences in their thermal expansion and composition, which can lead to cracking or poor fusion.[31] Welding reigns supreme as the preferred method for joining both similar and dissimilar metals, especially when aiming for high productivity in large-scale projects like oil pipelines. This often involves using a significant amount of heat input to achieve strong and efficient connections.[4] To ensure precise and reliable welds in critical applications, researchers are refining conventional arc welding techniques to minimize, or even eliminate, the heat-affected zone (HAZ) and reduce dependence on high-energy beam processes. CMT welding is a revolutionary TIG/MIG technique that reinvents droplet transfer. Unlike traditional dip transfer, where current plays a major role, CMT relies on wire retraction for droplet release. This unique approach, characterized by rapid shifts between arc ignition and cooling, significantly reduces heat input and minimizes workpiece strain.[5] CMT shines compared to traditional MIG welding by being energy-efficient, spatter-free, and surprisingly fast. It conquers the challenge of welding thin sheets. However, incomplete fusion lurks as a danger, particularly in lap joints.[6]

Investigating the impact of welding parameters on the strength of thin AISI 304 stainless steel sheets, Ghosh et al. conducted a meticulous study using the cold metal transfer technique. Specifically, their findings revealed the welding speed as the most crucial factor, with higher speeds leading to enhanced weld strength.[7] Literature shows that CMT welding has the potential of joining previously impossible combinations of dissimilar stainless steels, thanks to its exceptional control and minimal heat impact. Choosing the right filler metal becomes crucial when welding dissimilar stainless steels, as their diverse physical, chemical and metallurgical properties pose unique challenges.[8] Balaram Naik et al. examined the welding of duplex stainless steel using the ER308L filler wire, which exhibits a higher ultimate tensile strength, hardness and toughness.[9] Austenitic stainless steel welded using the ER308 L filler wire exhibits higher mechanical properties than 316L and 310 filler wire.[10] Austenitic and Duplex stainless steel joints with ER308L achieve the best pitting corrosion resistance.[11] The ER 308 L filler wire provides better mechanical and corrosion properties in welding dissimilar stainless steel. Specific control of parameters like current, welding speed (travel speed) and CTWD in CMT welding reveals superior weld strength and consistency, making it suitable for a wider range of applications. This adaptability, coupled with increased productivity, drives the ongoing research of parameter optimization techniques.[7] G. S. Vinodkumar et al. studied multi-objective optimization of solid state welded 430 steel joints whose joint strength was improved using the integrated grey and RSM approach.[12] Pratiwi et al. studied the effects of shielded metal arc welding parameters on dissimilar joints between AISI 316L and A36M steel using a GRA-Taguchi approach. Their analysis revealed a significant influence of all the investigated parameters (filler metal type, heat input current, arc gap voltage, and travel speed) on the joint's hardness, tensile strength, and flexural strength.[13] Kannan et al. found that for CMT welding of AISI 316L thin sheets for tailor welded blanks applications, the optimal settings involved reducing the speed to 300 mm/min while increasing the current to 105 A.[14] Luchtenberg et al. studied the heat input impact on S32205 duplex stainless steel welded with CMT, finding that it alters the ferrite/austenite balance: higher heat promotes intergranular austenite and hinders the ferrite formation.[15] Literature reveals the optimization of welding processes through experimentation, enhancing material characteristics and mechanical properties.

This research proposes a hybrid approach combining the Taguchi method and the TOPSIS technique to address these limitations. The Taguchi method efficiently identifies promising parameter combinations through its orthogonal array design, reducing the experimental workload. Subsequently, the TOPSIS technique precisely selects the optimal setting based on multiple performance criteria. It also determines the optimal process parameters by calculating the relative closeness to the ideal solution.[16] Available literature documents extensive research devoted to process parameter optimization and model development. However, there is a notable scarcity of studies specifically focused on the parametric optimization of dissimilar joints composed of Duplex 2205 and SS301LN stainless steel. Recognizing the success of computational methods in other applications, this research addresses this gap by applying an integrated Taguchi-TOPSIS approach to optimize process parameters for CMT welding of these dissimilar materials and develop quality weld joints. Optimal parameters for dissimilar weld joints were determined through a micro-

Table 1: Elemental composition of the base materials and the filler wire

Materials	Fe	C	Mn	Si	Cr	Mo	Ni	Cu	N
SS301LN	73.131	0.02	1.35	0.51	17.23	0.15	6.79	0.29	0.035
Duplex 2205	65.961	0.02	1.28	0.29	22.83	2.94	5.81	0.28	0.148
ER308L	Bal	0.02	1.42	0.42	19.15	0.25	10.03	0.21	0.054

Figure 1: CMT welding set-up

Table 2: Welding process parameters and their corresponding levels

Control variable	Current *I* (A)	Welding speed (mm/sec)	CTWD (mm)
L 1	85	4	3
L 2	90	6	5
L 3	95	8	7

structure examination, utilizing Taguchi's L9 design for efficient data collection.

2 MATERIALS AND METHODS

2.1 Materials

The study focuses on two base metals, namely SS 301 LN and Duplex 2205, with the aim of creating an efficient joint using a 1.2 mm diameter ER 308L SS filler wire during cold metal transfer welding. To facilitate the welding process, rectangular specimens measuring 15 × 10 × 0.2 cm were extracted from both plates using wire electric discharge machining (WEDM). In order to ensure that the carbon content and composition of the candidate materials aligned with the ASTM E1086-14 standards, optical emission spectrometry was performed. Chemical composition information for the SS plates and filler material can be found in **Table 1**.

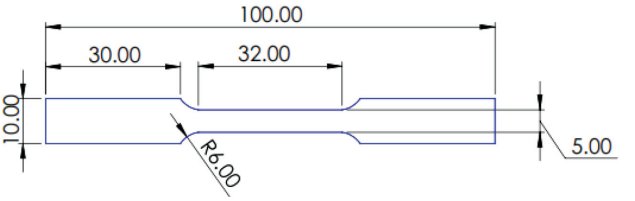

Figure 3: Tensile test specimen

The experiments were conducted using a FRONIUS TPS 400i CMT robotic welding machine, and **Figure 1** depicts the set-up used in the experimental process. Throughout the welding process, a visual inspection was conducted to assess the quality of the weldments. It was ensured that all welds were free of visible defects such as surface porosity and blowholes, resulting in a consistent and satisfactory weld geometry. **Table 2** depicts the selected welding parameters and their respective levels, determined by combining two approaches: screening experiments and consulting the American Welding Society (AWS) handbook. Each parameter was distributed equally across three levels. After conducting the robotic welding process, welded plates were cut into two samples, one for the tensile test and the other for microhardness and metallographic examinations.

The microstructure analysis was performed using an optical microscope from DEWINTER Optical Inc., followed by the standard metallographic procedure for preparing the test specimens. The microhardness of the welded joint samples was assessed using a Vickers microhardness tester (HDNS-Kelly Instruments) with an applied load of 500 gm for 10 s. Tensile tests were conducted on the prepared specimens, following the ASTM: E8/E8M-011 standards, using a universal testing machine (UTM) (Associated Scientific Eng. Works, New Delhi) with a speed of 1 mm/min. Specimens with a

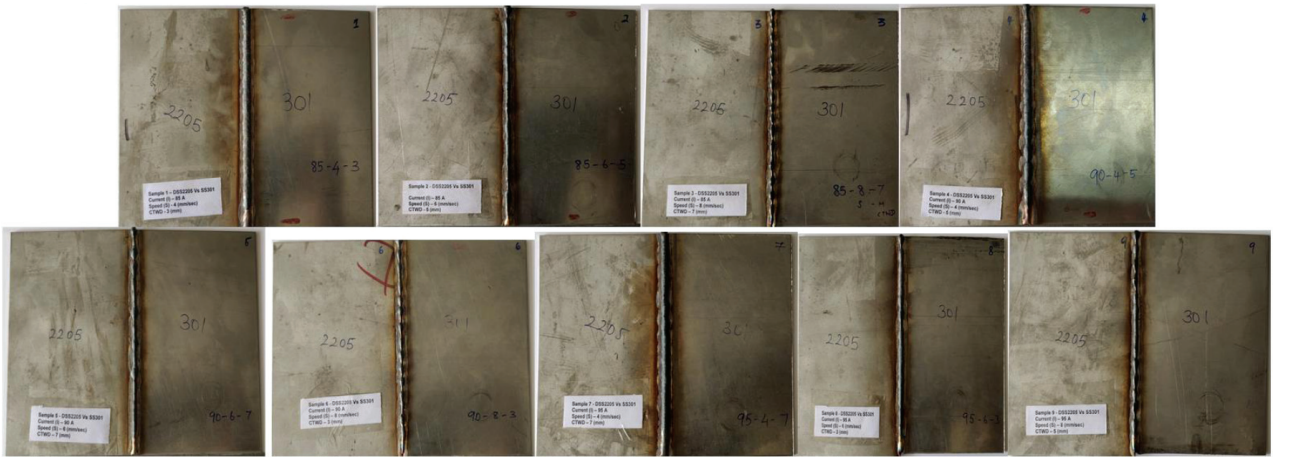

Figure 2: CMT welded specimens

gauge length of 25 mm were prepared, as depicted in **Figure 3**. Cross-sections and fractured ends of the tensile specimens were analyzed using a Carl Zeiss-Sigma 300 field emission scanning electron microscope (FESEM) to assess the nature of the welded joints.

2.2 Design of experiments

2.2.1 Taguchi method

The Taguchi method provides a systematic and efficient strategy for improving design performance, quality, and cost-effectiveness. It facilitates the optimization of quality characteristics through a precise adjustment of process parameters, while also reducing the system's sensitivity to variations in performance.[33] However, despite its extensive use for single-objective optimization in engineering, the Taguchi method faces challenges when addressing difficulties with multiple response variables due to its inherent limitations[17]. The development of advanced methodologies is crucial for effectively optimizing engineering problems with multiple performance characteristics.[18–20]

SN ratio for the higher-the-better criterion =

$$= -10 \log \frac{1}{x} \sum \frac{1}{y_{ij}^2} \quad (1)$$

Here, n represents the number of replicated measurements and y_{ij} denotes the i-th observation within the j-th replicate. Aiming to improve weldability, this study optimized welding parameters through a two-pronged approach, maximizing both ultimate tensile strength (UTS) and hardness (HR). Utilizing Equation (1), an S/N ratio analysis quantified parameter effects on these objectives. Subsequently, the Taguchi analysis, conducted in Minitab 17.0, employed "mean of means" and "mean of S/N ratio" plots along with ANOVA to statistically identify significant influencing factors. Insights collected from these analyses are detailed in **Table 3** and the following sections.

2.3 Multi-objective optimization

2.3.1 Technique for order preference by similarity to ideal solution (TOPSIS)

When making complex manufacturing decisions, TOPSIS empowers informed choices by evaluating parameter sets based on multiple criteria and their importance. This method identifies the optimal set by minimizing the distance to the "perfect scenario" and maximizing the distance to the "worst-case scenario" for all criteria.[21]

Stage 1: In TOPSIS, the initial data, captured in a decision matrix (n refers to attributes and m refers to alternatives), lays the foundation for evaluating and ranking potential solutions.[22]

$$D_{\mathrm{m}} = \begin{bmatrix} x_{11} & x_{12} & x_{13} & \cdots & \cdots & x_{1n} \\ x_{21} & x_{22} & x_{23} & \cdots & \cdots & x_{2n} \\ x_{31} & x_{32} & x_{33} & \cdots & \cdots & x_{3n} \\ \vdots & \vdots & \vdots & \ddots & \ddots & \vdots \\ \vdots & \vdots & \vdots & \ddots & \ddots & \vdots \\ x_{m1} & x_{m2} & x_{m3} & \cdots & \cdots & x_{mn} \end{bmatrix} \quad (2)$$

Stage 2: The equation below demonstrates how to produce a normalized matrix:

$$r_{ij} = \frac{x_{ij}}{\sqrt{\sum_{i=1}^{m} x_{ij}^2}}, j = 1,\ 2, ..., n \quad (3)$$

Stage 3: Each attribute weight is designated as wj, where j ranges from 1 to n. Employing these weights, the weighted regularized decision matrix V can be derived through ϑ_{ij}

$$V = \omega_j r_{ij} \quad (4)$$

where $\sum_j^n \omega_j = 1$

Step 4: Positive and negative values that satisfy the equation can be derived from the following terms:

$$V^+ = \left\{ \left(\sum_i^{\max} \vartheta_{ij} \middle| j \in J \right), \left(\sum_i^{\min} \middle| j \int J | i = 1,2,3,\ldots m \right) \right\} \quad (5)$$

$$= \vartheta_1^+, \vartheta_2^+, \vartheta_3^+, \ldots, \vartheta_n^+$$

$$V^+ = \left\{ \left(\sum_i^{\min} \vartheta_{ij} \middle| j \in J \right), \left(\sum_i^{\max} \middle| j \int J | i = 1,2,3,\ldots m \right) \right\} \quad (6)$$

$$= \vartheta_1^-, \vartheta_2^-, \vartheta_3^-, \ldots, \vartheta_n^-$$

Stage 5: The separation between changes is determined. The separation of each substitute from the "ideal" solution is given by

$$S_i^+ = \sqrt{\sum_{j=1}^{n} (\vartheta_{ij} - \vartheta_j^+)^2}, i = 1,2,3\ldots m \quad (7)$$

The separation of each alternative from the "negative ideal" solution is given by

$$S_i^- = \sqrt{\sum_{j=1}^{n} (\vartheta_{ij} - \vartheta_j^-)^2}, i = 1,2,3\ldots m \quad (8)$$

Stage 6: The comparative familiarity of a specific alternative to the ideal solution is expressed as

$$C_i = \frac{S_i^-}{S_i^+ + S_i^-}, i = 1,2,3\ldots m \quad (9)$$

Stage 7: Ranking the C_i values in descending order allows for the identification of both the most and least desirable alternative solutions. In the current study, the C_i multi-objective performance index can be optimized using the Taguchi method.

3 RESULSTS AND DISCUSSIONS

The experimental results for the Taguchi L9 orthogonal array is presented in the **Table 7**. The mechanical properties including the tensile strength and microhardness of dissimilar welds were analyzed using Minitab

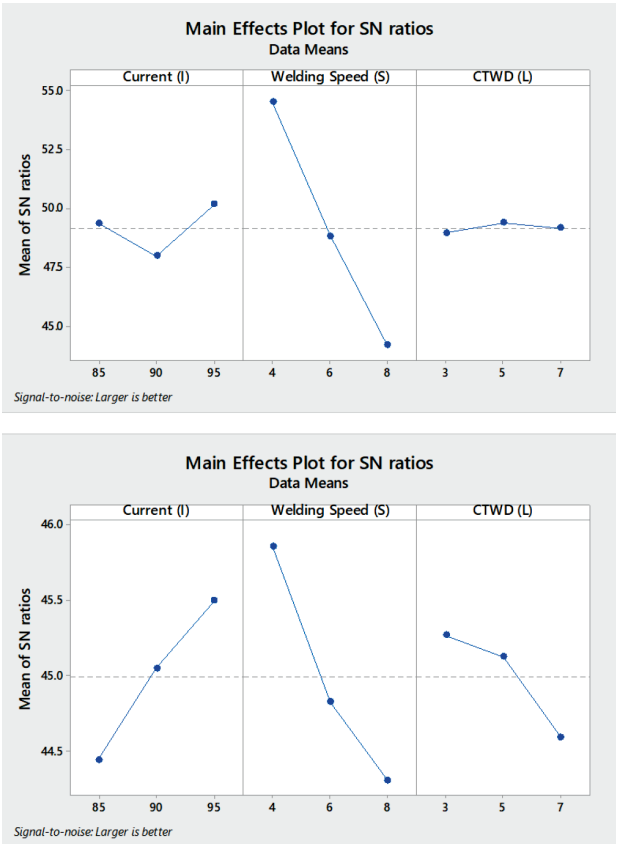

Figure 4: Effect of process parameters on UTS and hardness

17.0 software to assess the effect of welding parameters on their performance. The impacts of process parameters for tensile strength and microhardness were estimated using the Taguchi and ANOVA analysis.

3.1 Impact of process parameters on ultimate tensile strength: a Taguchi method

Figure 4 illustrates the effect of process parameters on the ultimate tensile strength (UTS). As shown, the UTS increases with the increasing current and decreasing welding speed. This is because a higher current provides more energy to the weld pool, resulting in a deeper penetration and a stronger joint. A slower welding speed gives the weld pool more time to cool down and solidify, which also reduces the risk of defects. The CTWD has a less significant effect on the UTS than the current and welding speed. However, the UTS is generally higher when the CTWD is short. This is because a shorter CTWD improves the arc stability and reduces spatter.

Table 3 shows the results of the S/N ratio analysis for the tensile strength obtained using the Taguchi method with MINITAB software. Among the welding parameters for CMT-joined dissimilar steels, the welding speed is supreme in influencing the tensile strength. The current plays a secondary role, with the contact tip-to-work distance having the minimal impact. Therefore, optimizing the welding speed becomes the key strategy for maximizing the tensile strength of these welds.

Table 3: Mean S/N ratio response table for ultimate tensile strength

Process parameters	Mean S/N ratio				
	L1	L2	L3	Delta	Rank
Current *I* (A)	49.38	47.97	50.17	2.2	2
Welding speed *S* (mm/sec)	54.51	48.83	44.18	10.32	1
CTWD *L* (mm)	48.96	49.39	49.17	0.43	3

3.2 Impact of process parameters on microhardness ($HV_{0.5}$): a Taguchi method

Figure 3 shows that $HV_{0.5}$ increases with increasing current and decreasing welding speed. This is because a higher current provides more energy to the weld pool, resulting in a finer grain structure and a harder weld. A slower welding speed gives the weld pool more time to cool down and solidify, which also increases $HV_{0.5}$. The CTWD has a smaller effect on $HV_{0.5}$ than the current and welding speed. However, $HV_{0.5}$ is generally higher when the CTWD is short. This is because a shorter CTWD provides better arc stability and reduces the risk of spatter. **Table 4** shows the results of the S/N ratio analysis for $HV_{0.5}$. The current is the most significant factor affecting $HV_{0.5}$, followed by the welding speed and CTWD. Hence, the current is the most crucial parameter for optimizing the microhardness of dissimilar steels welded with CMT.

Table 4: Mean S/N ratio response table for microhardness

Process parameters	Mean S/N ratio				
	L1	L2	L3	Delta	Rank
Current *I* (A)	44.44	45.05	45.49	1.05	2
Welding speed *S* (mm/sec)	45.86	44.82	44.3	1.55	1
CTWD *L* (mm)	45.27	45.12	44.59	0.68	3

Table 5: ANOVA of ultimate tensile strength

Source	DF	Seq SS	Adj SS	Adj MS	F	P	% contribution
Current *I*	2	7.447	7.447	3.7233	5.25	0.160	4.39
Welding speed *S*	2	160.373	160.373	80.1867	113.10	0.009	94.61
CTWD *L*	2	0.275	0.275	0.1375	0.19	0.838	0.16
Residual error	2	1.418	1.418	0.7090			0.84
Total	8	169.513					100

Table 6: ANOVA of microhardness ($HV_{0.5}$)

Source	DF	Seq SS	Adj SS	Adj MS	F	P	% contribution
Current *I*	2	1.6726	1.6726	0.83629	14.36	0.065	26.57
Welding speed *S*	2	3.7455	3.7455	1.87277	32.17	0.030	59.50
CTWD *L*	2	0.7608	0.7608	0.38038	6.53	0.133	12.09
Residual error	2	0.1164	0.1164	0.05822			1.85
Total	8	6.2953					100

Table 7: Experimental plan, experimental results and their calculated S/N ratios

S. No	Current (A)	Welding Speed (mm/sec)	CTWD (mm)	UTS MPa	$HV_{0.5}$	SN ratio for UTS	SN ratio for Hardness
1	85	4	3	566.24	193.56	55.0600	45.7363
2	85	6	5	282.28	164.50	49.0136	44.3233
3	85	8	7	159.64	145.60	44.0628	43.2632
4	90	4	5	457.28	198.45	53.2036	45.9530
5	90	6	7	256.54	170.45	48.1831	44.6319
6	90	8	3	133.77	168.90	42.5272	44.5526
7	95	4	7	578.95	196.70	55.2528	45.8761
8	95	6	3	291.84	188.56	49.3029	45.5090
9	95	8	5	198.54	179.76	45.9570	45.0939

3.3 ANOVA for ultimate tensile strength (UTS) and microhardness ($HV_{0.5}$)

Analysis of variance (ANOVA) identified the process parameters with the most significant influence on the performance characteristics. This was achieved by decomposing the total variability of multiresponse signal-to-noise ratios into contributions from individual process parameters and error terms. **Tables 5** and **6** present the ANOVA results for the ultimate tensile strength (UTS) and microhardness ($HV_{0.5}$). These results reveal that the welding speed exerted the strongest influence on both UTS and $HV_{0.5}$, followed by the current and CTWD, respectively. Individual contributions of these parameters to the UTS were quantified as 4.39 % for the welding speed, 94.61 % for the current and 0.16 % for the CTWD. Similarly, to $HV_{0.5}$, the welding speed contributed 32.46 %, the current 55.77 %, and the CTWD 9.76 %. These findings highlight the dominant role of the welding speed in affecting both the UTS and $HV_{0.5}$.

The quality of individual responses is assessed through S/N ratios, ensuring that valuable information stands out from irrelevant details. The obtained S/N ratio response for the UTS and microhardness is shown in **Tables 3** and **4**. Higher S/N ratios indicate superior quality characteristics and also represent the smallest difference between the required and measured output. From **Tables 3** and **4**, it is clear that the highest mean S/N ratio obtained for UTS is 55.25 at Level 3 – a current of 95 A, Level 1 – a welding speed of 4 mm/sec and Level 2 – a CTWD of 5 mm. For microhardness, the highest values are observed at Level 3 – a current of 95 A, Level 1 – a welding speed of 4 mm/sec and Level 2 – a CTWD of 3 mm. The welding efficiency, calculated as the ratio of the tensile strength of the weld joint to the base material, was approximately 93 %. Therefore, the optimum process parameters for achieving a high ultimate tensile strength and hardness during CMT welding were successfully predicted using the Taguchi method.

3.4 Multi-response optimization based on TOPSIS

This study employed TOPSIS to enhance the CMT welding process while considering multiple performance

Table 8: Performance index with the rank order

Expt. No	Normalized matrix		Weighted normalized decision matrix		Euclidean distance		Si + Si	Ci	Rank
			Si+	Si-					
1.	0.3718	0.3388	0.7436	0.6776	0.0041	0.1705	0.1747	0.97635	2
2.	0.3310	0.3283	0.6619	0.6566	0.0876	0.0876	0.1752	0.49985	5
3.	0.2975	0.3205	0.5951	0.6409	0.1563	0.0260	0.1823	0.14269	8
4.	0.3593	0.3404	0.7185	0.6808	0.0277	0.1462	0.1739	0.84084	3
5.	0.3254	0.3306	0.6507	0.6612	0.0975	0.0765	0.1740	0.43981	6
6.	0.2872	0.3300	0.5743	0.6600	0.1731	0.0034	0.1765	0.01923	9
7.	0.3731	0.3398	0.7462	0.6796	0.0011	0.1734	0.1745	0.99347	1
8.	0.3329	0.3371	0.6658	0.6742	0.0806	0.0932	0.1738	0.53611	4
9.	0.3103	0.3340	0.6206	0.6680	0.1262	0.0477	0.1739	0.27433	7

Table 9: ANOVA for TOPSIS performance index

Source	Deg F	Seq SS	Adj SS	Adj MS	F	P	% influence
Current *I*	2	0.044384	0.022192	7.64	0.116	0.0443	4.48
Welding speed *S*	2	0.940006	0.470003	161.89	0.006	0.9400	94.79
CTWD *L*	2	0.001456	0.000728	0.25	0.8	0.0014	0.15
Residual error	2	0.005806	0.002903			0.0058	0.59
Total	8	0.991652				0.9916	
S = 0.0538814	R – Sq = 99.41 %	R – Sq (adj) = 97.66 %					

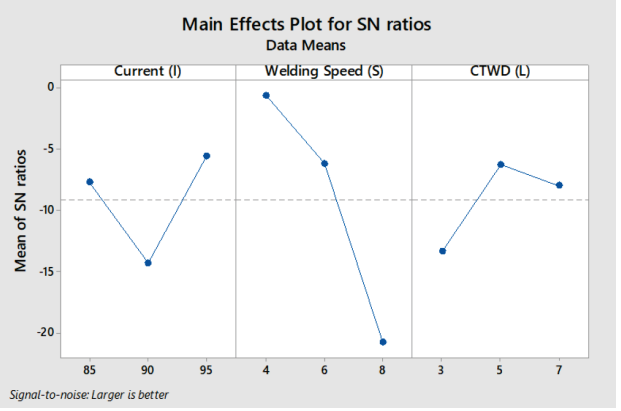

Figure 5: SN ratio for TOPSIS performance index

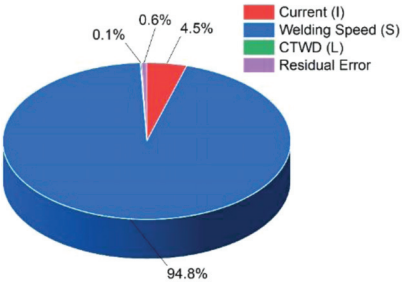

Figure 6: Percentage contribution of process parameters

characteristics, namely the ultimate tensile strength (UTS) and microhardness ($HV_{0.5}$). By analyzing the results of experimental runs, TOPSIS assigned a preference value to each combination of settings. These preference values reflected the relative closeness of each combination to the ideal solution, calculated as the ratio of the negative ideal separation measure to the sum of both positive and negative ideal separation measures. This approach effectively transformed the multi-criteria optimization problem into a single-objective problem. **Table 7** presents the signal-to-noise (SN) ratios for UTS and microhardness ($HV_{0.5}$), while **Table 8** details the calculated preference values and the resulting ranking order for each experimental run using Equations (2)–(8). The experimental run with the highest preference value and rank, indicating the closest proximity to the ideal solution, represents the optimal process settings and delivers the best overall performance. Experiment 7 demonstrates a higher tensile strength, confirming a strong joint without compromising the integrity of the welded region. During testing, the material typically fractured within the base metal (BM), indicating that both the weld and the heat-affected zone (HAZ) were stronger than the BM.

Using multi-objective TOPIS techniques, the optimum process parameters with their levels are determined with higher levels of relative closeness values, which include a current of 95 A, welding speed of 4 mm/sec and CTWD of 7 mm for dissimilar stainless steel joints. **Table 8** shows the performance index list for the relative closeness values and their ranks.

3.5 ANOVA for TOPSIS

Analysis of variance (ANOVA) revealed that the TOPSIS performance index (Ci) was significantly influenced by the welding speed, followed by current and CTWD. The welding speed had the highest impact, contributing 94.79 % to Ci variations, while the current and CTWD contributed 4.48 % and 0.15 %, respectively, as shown in **Table 9**. This confirms the dominant role of welding speed, affecting the overall performance. A further analysis using signal-to-noise (SN) ratio plots generated by Minitab software (**Figure 5**) supported this observation, showing a clear trend of an increasing performance index with higher welding speed and current. The minimal influence of the CTWD is also evident. **Table 10** lists the specific welding parameters with significant contributions to enhancing the preference solution value. The predicted optimal settings for maximizing Ci are a current of 95 A, welding speed (travel speed) of 4 mm/sec and CTWD of 5 mm. The influencing process parameter contributions to the TOPSIS multi-objective optimization approach are illustrated in **Figure 6**.

Table 10: Response table for signal-to-noise ratios

Level	Current *I*	Welding speed *S*	CTWD *L*
1	–7.7461	–0.6078	–13.3432
2	–14.3246	–6.1925	–6.2613
3	–5.5503	–20.8206	–8.0164
Delta	8.7743	20.2129	7.082
Rank	2	1	3

3.6 Confirmatory experiment for TOPSIS

By applying the multi-objective optimization approach, it was found that the welding speed significantly

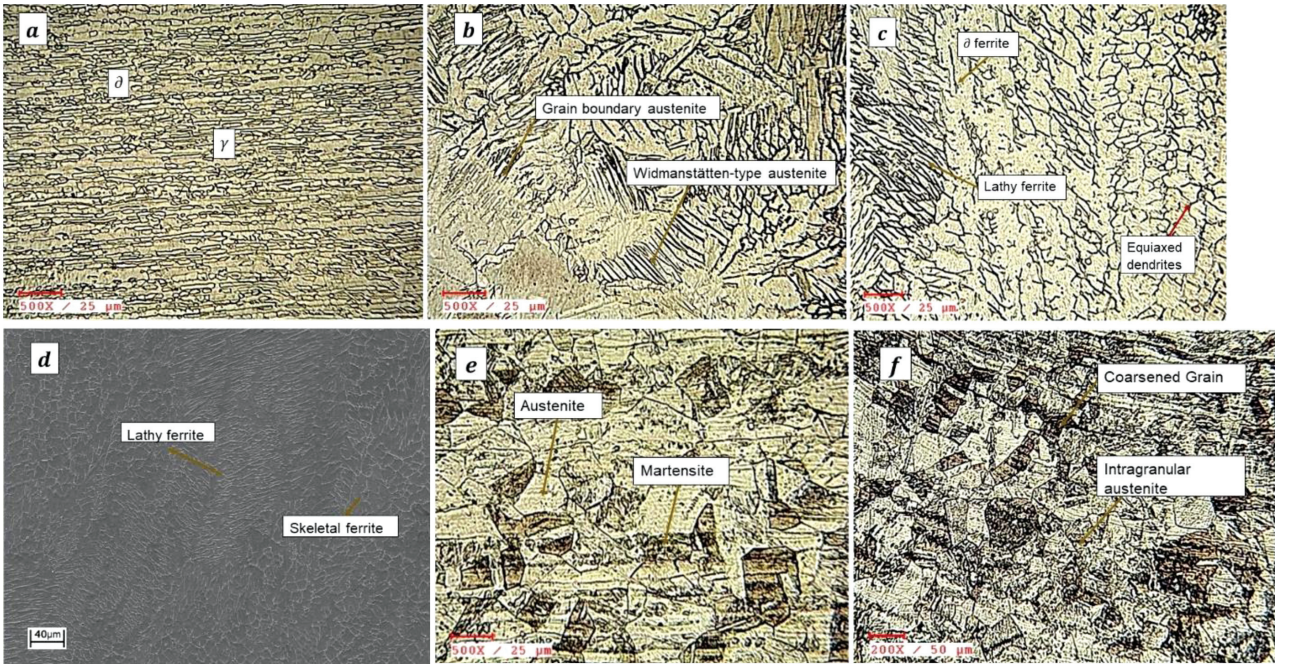

Figure 7: Microstructure of optimized dissimilar CMT welded specimen with different weld regions: a) 2205 base metal, b) 2205 HAZ, c) OM weld zone, d) SEM weld zone, e) 301LN base metal, f) 301LN HAZ

influences the weld strength. A regression equation was generated using performance index values (Ci). Confirmation tests were conducted to validate the optimal control factors obtained during the investigation. These optimal settings were determined with the Taguchi method based on the developed regression model. For the predicted optimal settings (a current of 95 A, welding speed of 4 mm/sec, CTWD of 5 mm), confirmation experiments were conducted, with the tensile strength and hardness calculated. The calculated percentage error between the actual and optimized welding parameters indicates a significant improvement in welding dissimilar stainless steel joints using the integrated Taguchi and TOPSIS optimization technique.

Table 11: Comparison of optimized welding parameter test results

Response	Mechanical properties		% error
	Actual	Optimized	
Level of factors	I95, S4, L7	I95, S4, L5	
Tensile strength	578.95	615.4	6.29
Microhardness	196.70	206.4	4.93

3.7 Microstructure analysis

Figure 7 indicates the microstructure of an optimized dissimilar CMT welded specimen with various weld regions. The 2205 base metal reveals the presence of a ferrite (δ) dark region and an austenite (γ) white region in **Figure 7a**.[23] The 301LN base metal shows the presence of a higher austenite phase and a martensite phase due to cold rolling.[24] The 2205 DSS weld interface exhibits a coarse, hardened grain structure due to its higher thermal conductivity in **Figure 7b**. The 301LN interface shows a hardened but less coarse structure due to its lower thermal conductivity in **Figure 7f**.[25] The OM and SEM analyses reveal that during welding, the weld metal forms a ferritic microstructure, as seen in **Figures 7c**, **7d**. As the temperature decreases further, a partial transformation into the austenitic phase occurs.[26,27] During welding, the weld metal nucleates into three different morphologies: Widmanstätten-type austenite, intragranular austenite and grain boundary austenite.[28] Both sides of the weld interface exhibit the presence of Widmanstätten-type austenite and intragranular austenite, as shown in **Figures 7b**, **7f**. The δ-ferrite is a key factor in predicting the solidification behavior and partitioning of chromium between ferrite and austenite in the weld zone.[14] **Figure 7c** indicates the presence of δ-ferrite, which increases the magnetic susceptibility of the weld metals. **Figure 7d** confirms the weld refinement and sufficient nucleation in the weld zone with the presence of equiaxed dendrites and two forms of ferrites. The two forms of ferrites, skeletal and lathy ferrite, are due to the ferrite-austenite transformation in the weld zone.[29]

During the CMT welding process, the filler material forms a metallurgical bond with the base metals, forming a homogeneous joint.[32] The findings confirm the absence of solidification cracking in dissimilar weld metals. However, no secondary phases are observed within the weld cap region. Furthermore, there is no evidence of an intermetallic phase formation in the HAZ region or chromium nitride formation within the weldments.

In the dissimilar welded zone energy-dispersive X-ray spectroscopy (EDXS) was performed and results are shown in **Figure 8** and **Table 12**. The EDXS analysis confirmed the presence of crucial alloying elements like chromium, nickel and molybdenum in the weld zone, en-

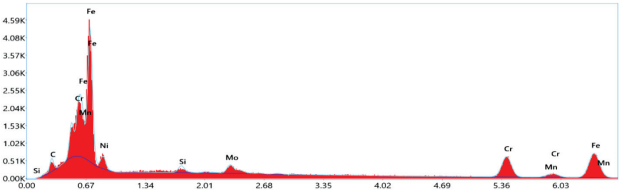

Figure 8: EDXS analysis of a CMT-welded dissimilar specimen

suring the consistency of dissimilar joints. No major compositional changes were observed in the weld, validating the quality of the fusion. There were no major changes in the weld metal composition, but there was a minor increase in the ferrite content in the weld metal due to the δ-ferrite content.[30]

Table 12: EDXS results for a CMT-welded dissimilar specimen

Element	C	Si	Cr	Mn	Fe	Ni	Mo
Weight %	3.74	1.17	39.14	4.63	42.48	4.53	4.31

4 CONCLUSION

This study investigated the production of quality joints, made with cold metal transfer (CMT) welding, including dissimilar stainless steel sheets, Duplex 2205 and SS 301 LN, using the ER 308L SS filler wire. The focus was on optimizing the welding parameters for maximizing the joint strength, specifically the ultimate tensile strength (UTS) and microhardness. The Taguchi L9 orthogonal array was used to find the most significant parameters among current, welding speed (travel speed) and contact-to-work distance (CTWD), and their optimum settings for achieving the highest strength values. The TOPSIS multi-objective optimization technique was employed to optimize the ultimate tensile strength (UTS) and microhardness ($HV_{0.5}$). The obtained results are as follows:

- The effects of process parameters and results of the S/N ratio analysis for ultimate tensile strength and microhardness were analysed using the Taguchi method. The welding speed played a major role in improving the ultimate tensile strength of the welded joints, while the welding current influenced the maximizing of the microhardness of the welded joints.
- The ANOVA results show that the highest mean S/N ratio obtained for the UTS is 55.25 at Level 3 – a current of 95 A, Level 1 – a welding speed of 4 mm/sec and Level 2 – a CTWD of 5 mm, while the highest values for microhardness are found at Level 3 – a current of 95 A, Level 1 – a welding speed of 4 mm/sec and Level 2 – a CTWD of 3 mm.
- Optimum process parameters are obtained using TOPSIS multi-objective optimization techniques with ideal relative closeness values at a current of 95 A, welding speed of 4 mm/sec and CTWD of 7 mm for dissimilar stainless steel joints.
- The ANOVA results are obtained for TOPSIS performance index Ci, which shows that the welding speed has the highest impact, contributing 94.79 % to Ci variations, while current and CTWD contribute 4.48 % and 0.15 %.
- Experiments were conducted to confirm the improvement in the optimized and actual experimental parameters. The results are satisfactory and close to the predicted optimized settings.
- The SEM analysis shows that there is no evidence of secondary phases, and the presence of fine dendrites indicates high-quality weld joints.
- The integrated Taguchi and TOPSIS method is an effective tool for optimizing welding parameters for CMT welding of dissimilar stainless steels, allowing the production of components with increased mechanical properties, decreasing the costs and advancing the performance in chemical and food processing industries.

5 REFERENCES

[1] J. Verma, R. V. Taiwade, Effect of welding processes and conditions on the microstructure, mechanical properties and corrosion resistance of duplex stainless steel weldments – A review, J. Manuf. Process., 25 (**2017**), 134–152, ISSN 1526-6125. doi:10.1016/j.jmapro.2016.11.003

[2] X. Li, W. Liu, X. Guo, Z. Zhang, Z. Song, Microstructure Evolution of Laser Welded 301LN and AISI 304 Austenitic Stainless Steel, Metall. Mater. Trans. A, 54 (**2023**) 4, 1186–1198, doi:10.1007/s11661-023-06973-6

[3] K. Kuwayama, Water tank built to last 60 years, Nickel Development Institute, 1994, https://www.nickelinstitute.org/~/Media/Files/TechnicalLiterature/WaterTankBuilttoLast60Years_14030_.pdf, 10

[4] Y. Yang, B. Yan, J. Li, J. Wang, The effect of large heat input on the microstructure and corrosion behaviour of simulated heat affected zone in 2205 duplex stainless steel, Corros. Sci., 53 (**2011**) 11, 3756–3763, ISSN 0010-938X. doi:10.1016/j.corsci.2011.07.022

[5] K. Furukawa, New CMT arc welding process – welding of steel to aluminium dissimilar metals and welding of super-thin aluminium sheets, Weld. Int., 20 (**2006**) 6, 440–445, doi:10.1533/wint.2006.3598

[6] S. Selvi, A. Vishvaksenan, E. Rajasekar, Cold metal transfer (CMT) technology – An overview, Defence Technol., 14 (**2018**) 1, 28–44, ISSN 2214-9147. doi:10.1016/j.dt.2017.08.002

[7] J. G. Roy, N. Yuvaraj, Vipin, Effect of welding parameters on mechanical properties of cold metal transfer welded thin AISI 304 stainless-steel sheets, Trans. Indian Inst. Metals, 74 (**2021**) 9, 2397–2408, doi:10.1007/s12666-021-02326-2

[8] C. R. Das, A. K. Bhaduri, G. Srinivasan, V. Shankar, S. Mathew, Selection of filler wire for and effect of auto tempering on the mechanical properties of dissimilar metal joint between 403 and 304L(N) stainless steels, J. Mater. Process. Technol., 209 (**2009**) 3, 1428–1435, doi:10.1016/j.jmatprotec.2008.03.053

[9] A. B. Naik, A. Chennakesava Reddy, V. Venugopal Reddy, Effect of process parameters of tungsten inert gas welding on welding of duplex stainless steels, Int. J. Res. Appl. Sci. Eng. Technol., 6 (**2018**) 1, 2818–2827, doi:10.22214/ijraset.2018.1388

[10] G. Kaur, D. Singh, J. S. Grewal, Effect of filler wire composition on joining properties of GTAW stainless steel 202, Proc. of the Inter. Conf. on Research and Innovations in Mechanical Engineering, Springer India, New Delhi, 2014, 191–200, doi:10.1007/978-81-322-1859-3_17

[11] B. Varbai, P. Bolyhos, D. M. Kemény, K. Májlinger, Microstructure and corrosion properties of austenitic and duplex stainless steel dis-

similar joints, Period. Polytech. Mech. Eng., 66 (**2022**) 4, 344–349, doi:10.3311/PPme.21007

[12] G. S. Vinodkumar, V. Mayavan, G. Rathinasabapathi, A. G. David, Optimization of process parameters for a solid-state-welded AISI 430 steel joint with the GRG reinforced response surface methodology, Mater. Tehnol., 57 (**2023**) 5, 485–494, doi:10.17222/mit.2023.873

[13] D. K. Pratiwi, A. Arifin, Gunawan, A. Mardhi, Afriansyah, Investigation of Welding Parameters of Dissimilar Weld of SS316 and ASTM A36 Joint Using a Grey-Based Taguchi Optimization Approach, J. Manuf. Mater. Process., 7 (**2023**) 1, 39, doi:10.3390/jmmp7010039

[14] A. R. Kannan, N. S. Shanmugam, S. A. Vendan, Effect of cold metal transfer process parameters on microstructural evolution and mechanical properties of AISI 316L tailor welded blanks, Int. J. Adv. Manuf. Technol., 103 (**2019**), 4265–4282, doi:10.1007/s00170-019-03856-2

[15] P. Luchtenberg, P. T. de Campos, P. Soares, C. A. H. Laurindo, O. Maranho, R. D. Torres, Effect of welding energy on the corrosion and tribological properties of duplex stainless steel weld overlay deposited by GMAW/CMT process, Surf. Coat. Technol., 375 (**2019**), 688–693, doi:10.1016/j.surfcoat.2019.07.072

[16] B. Singaravel, B. Chakradhar, D. Soundar Rajan, A. Kiran Kumar, Optimization of friction stir welding process parameters using MCDM method, Materials Today: Proceedings, 76 (**2023**) 3, 597–601, doi:10.1016/j.matpr.2022.12.095

[17] G. Taguchi, System of Experimental Design: Engineering Methods to Optimize Quality and Minimize Cost, White Plains, UNIPUB/Kraus International, 1987

[18] H. I. Kurt, M. Oduncuoglu, N. F. Yilmaz, E. Ergul, R. Asmatulu, A Comparative Study on the Effect of Welding Parameters of Austenitic Stainless Steels Using Artificial Neural Network and Taguchi Approaches with ANOVA Analysis, Metals, 8 (**2018**), 326, doi:10.3390/met8050326

[19] K. Nandagopal, C. Kailasanathan, Analysis of mechanical properties and optimization of gas tungsten arc welding (GTAW) parameters on dissimilar metal titanium (6Al4V) and aluminium 7075 by Taguchi and ANOVA techniques, Journal of Alloys and Compounds, 682 (**2016**), 503–516, doi:10.1016/j.jallcom.2016.05.006

[20] S. Pandiarajan, S. Senthil Kumaran, L. A. Kumaraswamidhas, R. Saravanan, Interfacial microstructure and optimization of friction welding by Taguchi and ANOVA method on SA 213 tube to SA 387 tube plate without backing block using an external tool, Journal of Alloys and Compounds, 654 (**2016**), 534–545, doi:10.1016/j.jallcom.2015.09.152

[21] S. J. Chen, C. L. Hwang, F. P. Hwang, Fuzzy multiple attribute decision making methods and applications, книга (1992)

[22] Lan Tian-Syung, Taguchi optimization of multi-objective CNC machining using TOPSIS, Information Technology Journal, 8 (**2009**) 6, 917–922

[23] M. Atif Makhdoom, A. Ahmad, M. Kamran, K. Abid, W. Haider, Microstructural and electrochemical behavior of 2205 duplex stainless steel weldments, Surfaces and Interfaces, 9 (**2017**), 189–195, doi:10.1016/j.surfin.2017.09.007

[24] A. Järvenpää, M. Jaskari, M. Keskitalo, K. Mäntyjärvi, P. Karjalainen, Microstructure and mechanical properties of laser-welded high-strength AISI 301LN steel in reversion-treated and temper-rolled conditions, Procedia Manufacturing, 36 (**2019**), 216–223, doi:10.1016/j.promfg.2019.08.028

[25] J. C. Lippold, W. A. Baeslack, I. Varol, Heat-affected zone liquation cracking in austenitic and duplex stainless steels, Welding Journal (USA), 71 (**1988**) 1

[26] Y. Han, Y. Zhang, H. Jing, Z. Gao, L. Xu, Z. Zhang, L. Zhao, Microstructure and Corrosion Studies on Different Zones of Super Duplex Stainless Steel UNS S32750 Weldment, Front. Mater., 7 (**2020**) 251, doi:10.3389/fmats.2020.00251

[27] V. Muthupandi, P. Bala Srinivasan, S. K. Seshadri, S. Sundaresan, Effect of weld metal chemistry and heat input on the structure and properties of duplex stainless steel welds, Materials Science and Engineering: A, 358 (**2003**) 1–2, 9–16, doi:10.1016/S0921-5093(03)00077-7

[28] Z. Zhang, Z. Wang, Y. Jiang, H. Tan, D. Han, Y. Guo, J. Li, Effect of post-weld heat treatment on microstructure evolution and pitting corrosion behavior of UNS S31803 duplex stainless steel welds, Corrosion Science, 62 (**2012**), 42–50, doi:10.1016/j.corsci.2012.04.047

[29] John C. Lippold, Damian J. Kotecki, Welding metallurgy and weldability of stainless steels, 2005

[30] G. Chandrasekar, C. Kailasanathan, D. K. Verma, et al., Optimization of welding parameters, influence of activating flux and investigation on the mechanical and metallurgical properties of activated TIG weldments of AISI 316 L stainless steel, Trans. Indian Inst. Met., 70 (**2017**), 671–684, doi:10.1007/s12666-017-1046-5

[31] A. Bhattacharya, R. Kumar, Dissimilar joining between austenitic and duplex stainless steel in double-shielded GMAW: a comparative study, Mater. Manuf. Process., 31 (**2016**) 3, 300–310, doi:10.1080/10426914.2015.1070414

[32] Mahmud Khan, M. W. Dewan, M. Z. Sarkar, Effects of welding technique, filler metal and post-weld heat treatment on stainless steel and mild steel dissimilar welding joint, J. Manuf. Process., 64 (**2021**), 1307–1321, doi:10.1016/j.jmapro.2021.02.058

[33] Y. S. Tarng, W. H. Yang, Optimisation of the weld bead geometry in gas tungsten arc welding by the Taguchi method, Int. J. Adv. Manuf. Technol., 14 (**1998**), 549–554, doi:10.1007/BF01301698